J Solid State Electrochem (2010) 14:1847–1854
DOI 10.1007/s10008-010-1044-6

ORIGINAL PAPER

Synthesis and electrochemical studies on LiV_3O_8

A. Sakunthala · M. V. Reddy · S. Selvasekarapandian · B. V. R. Chowdari · H. Nithya · P. Chirstopher Selvin

Received: 5 November 2009 / Revised: 2 March 2010 / Accepted: 5 March 2010 / Published online: 6 April 2010

Abstract The compound, lithium trivanadate (LiV_3O_8), was synthesized by the polymer precursor method, using the polymer polyvinylpyrrolidone. The electrochemical performance of LiV_3O_8 was compared with LiV_3O_8 synthesized by the solid state reaction method. The prepared compounds were characterized by X-ray diffraction, scanning electron microscopy, and high-resolution transmission electron microscopy techniques. The electrochemical performances were studied by cyclic voltammetry and galvanostatic cycling in the voltage range of 2.0 to 4.0 V at room temperature (25 °C). The compound prepared by the polymer precursor method was found to have a good cycling stability. A reversible capacity value of 203 mAh/g (2.18 mol of Li) and 170 mAh/g (1.83 mol of Li) was obtained at the end of the 70th cycle, at a current density of 30 and 120 mA/g, respectively.

Keywords Lithium trivanadate · Cathode · Electrochemical studies · Cycling stability

A. Sakunthala · M. V. Reddy (✉) · B. V. R. Chowdari
Department of Physics, National University of Singapore, Singapore, 117542, Singapore
e-mail: phymvvr@nus.edu.sg

B. V. R. Chowdari
e-mail: phychowd@nus.edu.sg

A. Sakunthala · S. Selvasekarapandian · H. Nithya
DRDO-BU, Center for Life Sciences, Bharathiar University, Coimbatore, India

P. Chirstopher Selvin
NGM College, Pollachi, Tamilnadu, India

S. Selvasekarapandian
Kalasalingam University, Krishnankoil, Virudhunagar, 626190, Tamil Nadu, India
e-mail: sekarapandian@yahoo.com

Introduction

Vanadium-based compounds like V_2O_5, V_6O_{13}, and LiV_3O_8 are considered as attractive cathode materials for the rechargeable lithium polymer batteries because of their low working voltage of ~3 V vs Li, which will not degrade the polymer electrolyte even at high temperatures [1]. Among the above compounds, LiV_3O_8 has been extensively researched as a cathode material for the past 20 years. The electrochemical performance of this material mainly depends on the method of preparation, starting materials, calcination temperature, and reaction time. LiV_3O_8 has been prepared by different methods like freeze drying [2], solution dispersion [3], flame pyrolysis [4], spray drying [5], etc. The cyclic stability of this compound is found to be very poor, and the capacity drops within 10 cycles, as reported in literature [4, 5], but few reports are also seen with good cyclic stability [3, 6]. In the present work, LiV_3O_8 compound was prepared by the polymer precursor method and solid state (SS) method. The electrochemical properties of the LiV_3O_8 compounds prepared by the above methods were discussed.

Synthesis and experimental

The compound LiV_3O_8 was prepared by the polymer precursor (PP) method as follows. Stoichiometric amount of lithium acetate (0.54 g, purity 99.9%; Alfa Aesar) and ammonium metavanadate (1.76 g, purity 99.5%; Fisher Scientific) were mixed with the polymer polyvinylpyrrolidone (PVP K40, molecular weight 40,000, Aldrich) which was already dissolved in 100 ml of distilled water. The total metal ion to polymer ratio was maintained as 1:1.5. The solution was further refluxed for 2 h at a temperature of 100 °C. The resultant solution was evaporated on a hot plate; the dry residue was heat treated at 550 °C for about 10 h in air at a

heating rate of 3 °C/min. The preparation was repeated by heating the dry residue at a faster heating rate of 20 °C/min under similar conditions. In the discussion part, the PP method stands only for the compound prepared at a slow heating rate unless it is mentioned. The metal ions were dispersed nicely in the polymer solution owing to the bonding nature of them with the oxygen atom in PVP $(C_6H_9NO)_n$ which acts like a capping agent to control the particle growth. The combustible nature of the polymer helps in the formation of LiV_3O_8 at a low temperature, when compared to the traditional solid state method. In case of the SS reaction method, the raw materials Li_2CO_3 and V_2O_5 were mixed well and finally heated at 680 °C for 13 h in air at a heating rate of 3 °C/min.

Phase purity of LiV_3O_8 powders were studied by X-ray diffractometer (XRD) (Philips X'PERT MPD unit with *C*u Kα radiation). Scanning electron microscope (SEM) measurements were made by JEOL JSM-6700F instrument. Transmission electron microscope (TEM) measurements were made by JEOL JEM-3010 (300 kV) instrument. Electrochemical studies were carried out with 2016-type coin cells. The electrodes were fabricated with the active material LiV_3O_8, Super P conductive carbon black, and binder (Kynar 2801) in the weight ratio of 70:15:15, *N*-methyl-pyrrolidone as a solvent to the binder. Etched Al-foil (20 μm) was used as the current collector. Lithium metal foil was the negative electrode (anode), and 1 M $LiPF_6$ in ethylene carbonate + dimethyl carbonate (1:1 volume ratio; Merck, Selectipur LP40) was used as the electrolyte. More details on the electrode fabrication were discussed in our previous study [7]. Cyclic voltammetry (CV) studies were made at a scan rate of 0.058 mV/s, and the galvanostatic studies with a current density of 30 and 120 mA/g are made in the voltage range of 2.0 to 4.0 V vs Li at room temperature. Electrochemical impedance spectroscopy (EIS) studies were carried out with Solartron Impedance/gain/phase analyzer (model SI 1255) coupled with a Potentiostat (SI 1268) at room temperature. The frequency was varied from 0.18 MHz to 3 mHz with an alternating current signal of amplitude 10 mV. The Nyquist plots (Z' vs $-Z''$) were collected and analyzed using Z-plot and Z-view software (Version 2.2, Scribner associates Inc., USA).

Results and discussion

Structure and morphology

The Rietveld-refined XRD patterns of LiV_3O_8 prepared by PP and SS methods are shown in Fig. 1a, b. The experimental XRD patterns were fitted with the reported monoclinic structure with the space group $P2_1/m$. The main lines were indexed. The lattice parameter values were

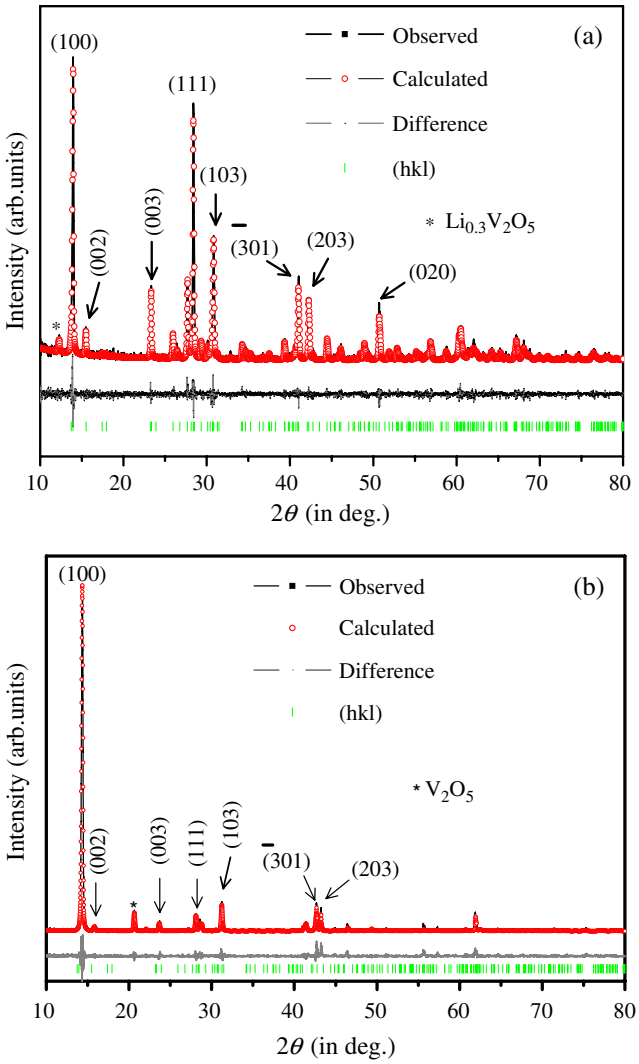

Fig. 1 Rietveld-refined XRD patterns of LiV_3O_8 prepared by **a** PP method and **b** SS method. Recorded with Cu Kα radiation. For clarity, only (hkl) lines corresponding to LiV_3O_8 phase are shown

calculated by the TOPAS software. The compound prepared by the PP method was found to have 98.2 wt.% of LiV_3O_8 main phase and 1.8 wt.% of $Li_{0.3}V_2O_5$ phase. The lattice parameter value of the main phase was found to be a=6.6566 (5) Å, b=3.5964 (3) Å, c=11.9964 (3) Å, and β =107.75°. The compound prepared by the SS method contains 97.8 wt.% of LiV_3O_8 and 2.2 wt.% of V_2O_5 phases. The lattice parameter value of the main phase are a =6.6562 (5) Å, b=3.6012 (3) Å, c=12.0079 (3) Å, and β= 107.75°. The major difference between the XRD patterns was the intensity of the peak corresponding to (100) hkl line over all the other peaks. It was found to be stronger in the case of the SS method when compared to the PP method. This showed that, for LiV_3O_8 prepared by SS method, the dimensions of the crystallites along the (100) plane was considerably larger than the out-of-plane directions due to preferred orientation. A similar kind of XRD

pattern of LiV_3O_8 compound prepared by the solid state method was reported by Wang et.al. [8]. The preferred orientation will lead to a relatively slow diffusion path for the lithium ions inserted between these planes [2]. SEM photograph of LiV_3O_8 show well-ordered layer plate-like morphology of LiV_3O_8 synthesized by the SS method (Fig. 2a), reflecting a very high crystalline nature, but for the PP method, the particles are found to have a definite rod-like morphology (Fig. 2b), with particle size in submicron range. In addition, TEM photograph (Fig. 2c) clearly shows the rod-like morphology of LiV_3O_8 (width<2 μm). The high-resolution image in the inset shows the lattice spacing corresponding to the (001) plane. Selected area electron diffraction (SAED) pattern in Fig. 2d shows the single crystalline nature of the particle.

The Rietveld-refined XRD pattern and the SEM image of the compound prepared by the PP method at a fast heating rate are shown in Fig. 3a, b, respectively. The obtained compound was found to have 57.08 wt.% of LiV_3O_8 phase, 34.38 wt.% of $Li_{0.3}V_2O_5$ phase, and 8.54 wt.% of V_2O_5 phase. The lattice parameter value of the LiV_3O_8 phase was a=6.6533 (5) Å, b =3.5979 (3) Å, c=12.0119 Å, and β=107.82°. The lattice parameter value of the other active phases, $Li_{0.3}V_2O_5$ and V_2O_5, were a=10.0788 (5) Å, b=3.6050 (3) Å, c=15.3804 Å, β=110.14° and a=11.5143 (5) Å, b=3.5653 (3) Å, c= 4.3767 Å, respectively. The compound with the high-impurity phase has been made to understand its influence on the electrochemical properties. The SEM image shows that the particles are submicron sized made of bundles of small rods (Fig. 3b).

Cyclic voltammetry

A comparison of the seventh cycle cyclic voltammogram of the compounds prepared by the PP and SS method are shown in the Fig. 4a. The peak currents were normalized with respect to their active mass. The observed main cathodic/anodic peak potentials in the voltammogram closely resemble for both the methods. A higher peak current value was obtained for the PP method leading to a higher reversible capacity as clearly reflected in galvanostatic cycling studies. The main anodic peaks around 2.8 and 2.9 V are due to the extraction of lithium from LiV_3O_8, and the two cathodic peaks around 2.7 and 2.8 V are due to the different energy sites available for the lithium insertion in a single phase reaction. The peak at 2.5 V vs Li is due to the filling of octahedral sites, where two phases co-exist [9, 10]. An anodic/cathodic peak around 3.4 V and a cathodic

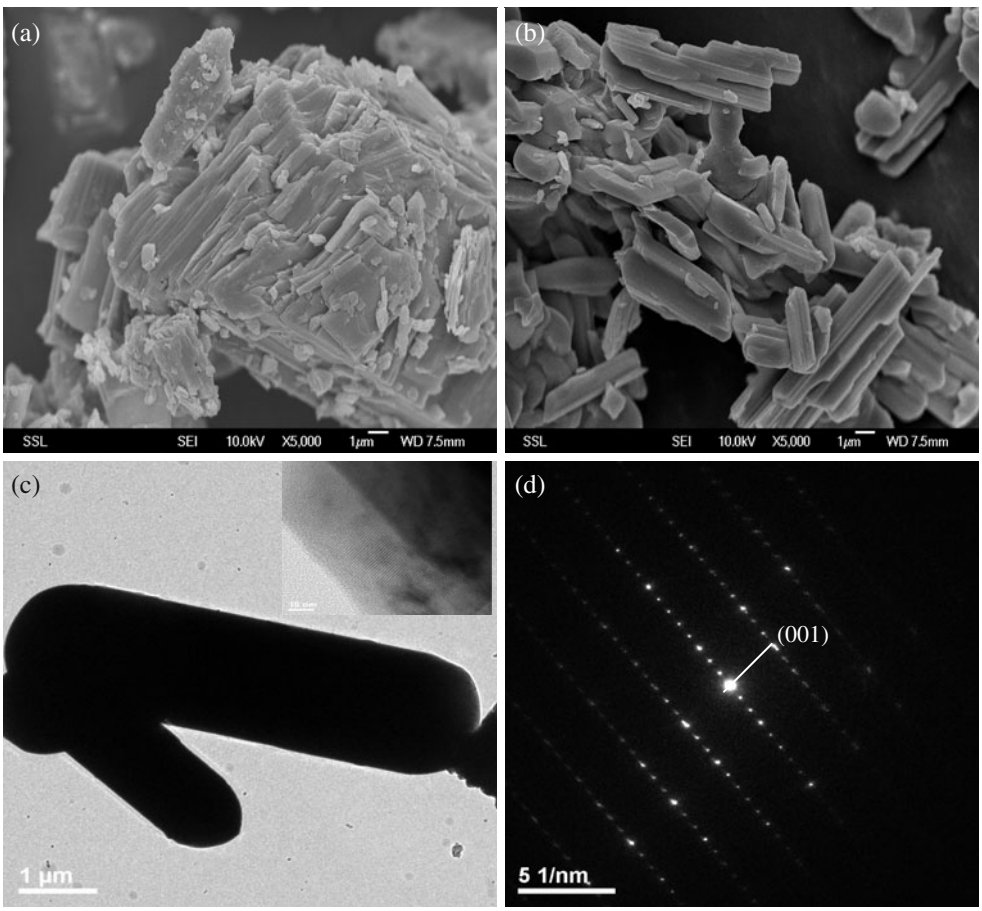

Fig. 2 SEM images of LiV_3O_8 by **a** SS method and **b** PP method. *Scale bar*, 1 μm (10 kV, ×5,000); **c** TEM images of LiV_3O_8 by PP method. *Scale bar*, 1 μm (*inset* high-resolution transmission electron microscopy image); and **d** SAED pattern

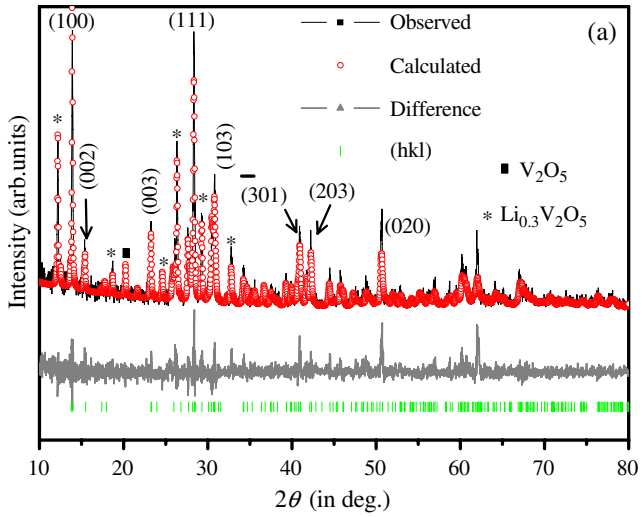

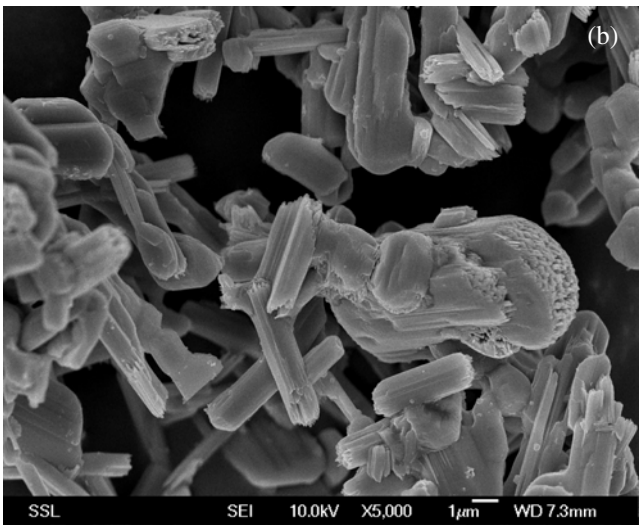

Fig. 3 **a** Rietveld-refined XRD pattern and **b** SEM image. *Scale bar*, 1 μm (10 kV, ×5,000) of the compound prepared by PP method at a fast heating rate. LiV_3O_8, $Li_{0.3}V_2O_5$, and V_2O_5 phases are shown in Fig. 3a

peak around 2.6 V (encircled) were observed for the compound prepared by the PP method. It is due to the impurity $Li_{0.3}V_2O_5$, an active phase for the electrochemical cycling [11]. A minor peak around 2.6 V was noticed for the compound prepared by the SS method.

Figure 4b shows the comparison of the second cycle cyclic voltammogram and the CV of the cell taken after 70 cycles of galvanostatic charge/discharge. During long-term cycling, the main anodic peak potential was shifted to lower values, indicating less energy for lithium extraction, and the peaks around 3.4 and 2.6 V observed during the second cycle are found to disappear.

Galvanostatic cycling

Figure 5a, b shows the galvanostatic discharge/charge curves of LiV_3O_8 prepared by the PP and SS methods. A

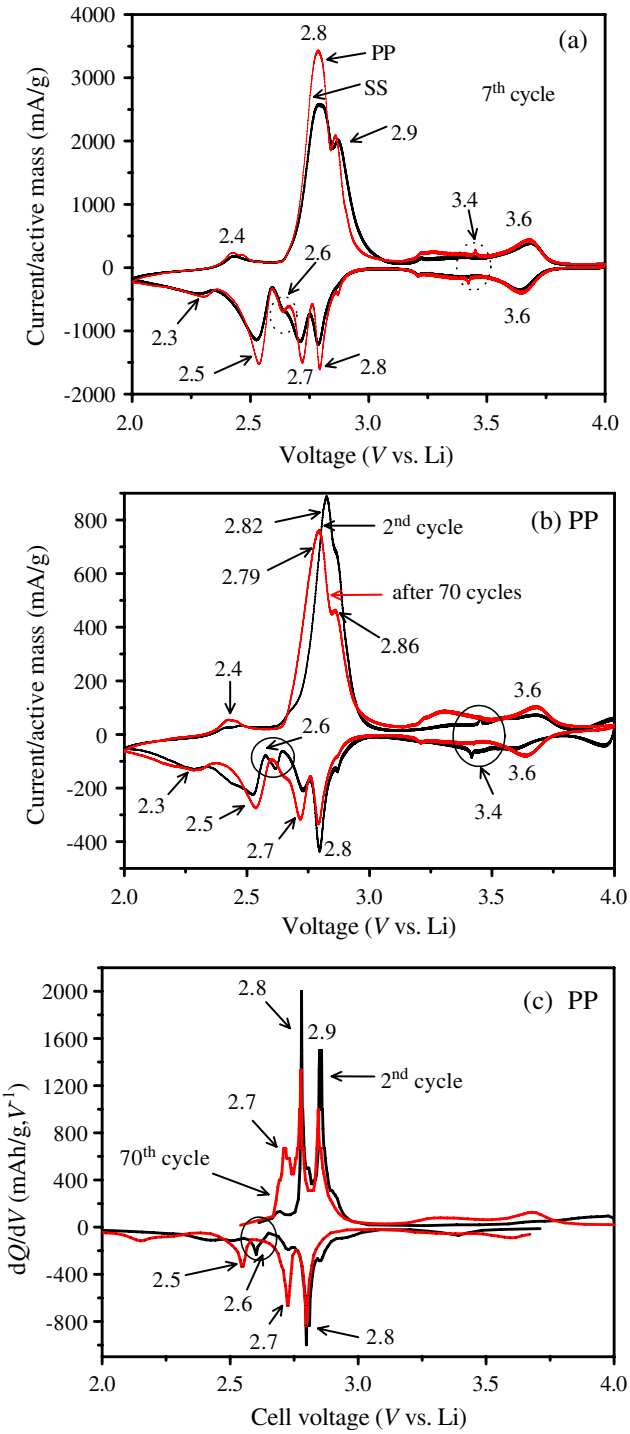

Fig. 4 Cyclic voltammogram of LiV_3O_8 at a scan rate of 0.058 mV/s and voltage range, 2.0 to 4.0 V, recorded at room temperature, **a** SS and PP method at seventh cycle, **b** PP method at second cycle and 70th cycle (after galvanostatic cycling studies), **c** 2nd and 70th cycle differential capacity vs voltage plots extracted from galvanostatic cycling (Fig. 5a)

good reversible plateau region around ~2.8 V was observed for both the compounds. The multiple plateaus observed in galvanostatic cycling are clearly reflected in the CV studies (Fig. 4a, b). The differential capacity vs voltage plot

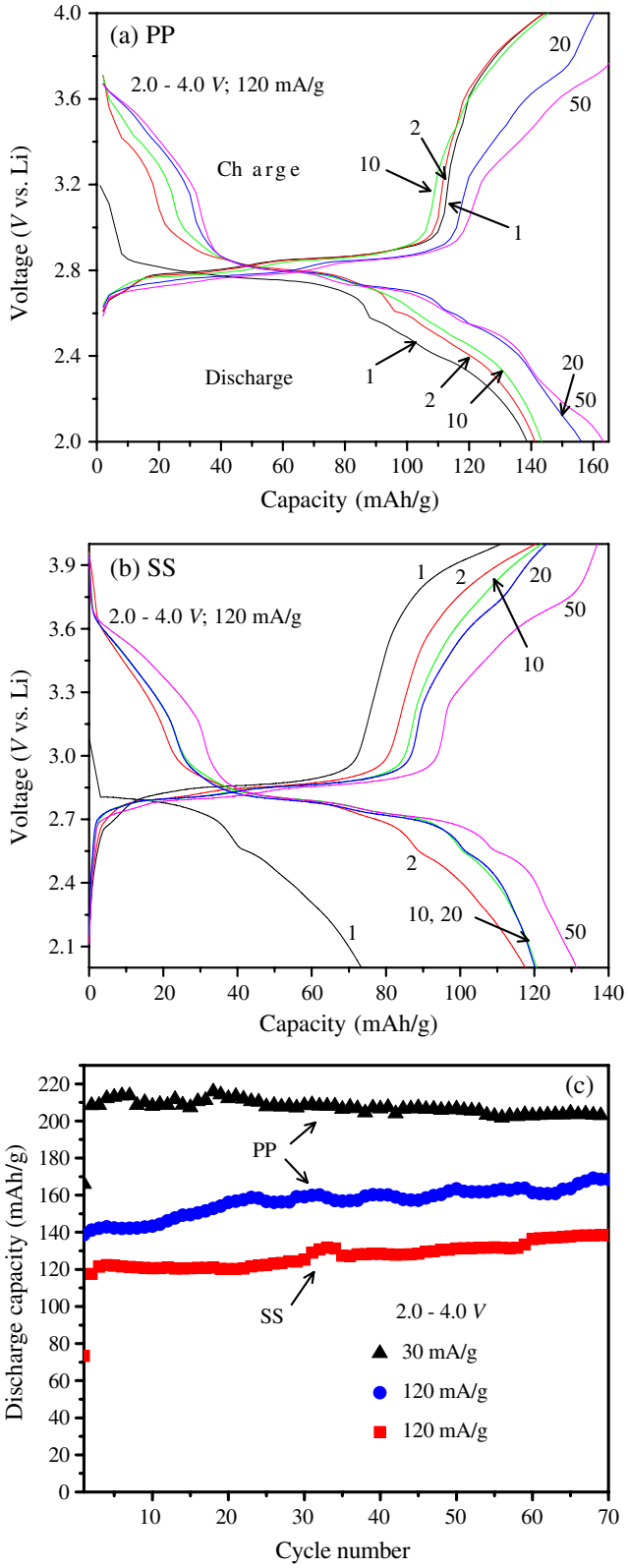

Fig. 5 Galvanostatic cycling voltage vs capacity profiles LiV_3O_8 of **a** PP method and **b** SS method; **c** capacity vs cycle number plots for the compounds prepared by PP and SS method. Voltage range, 2.0–4.0 V

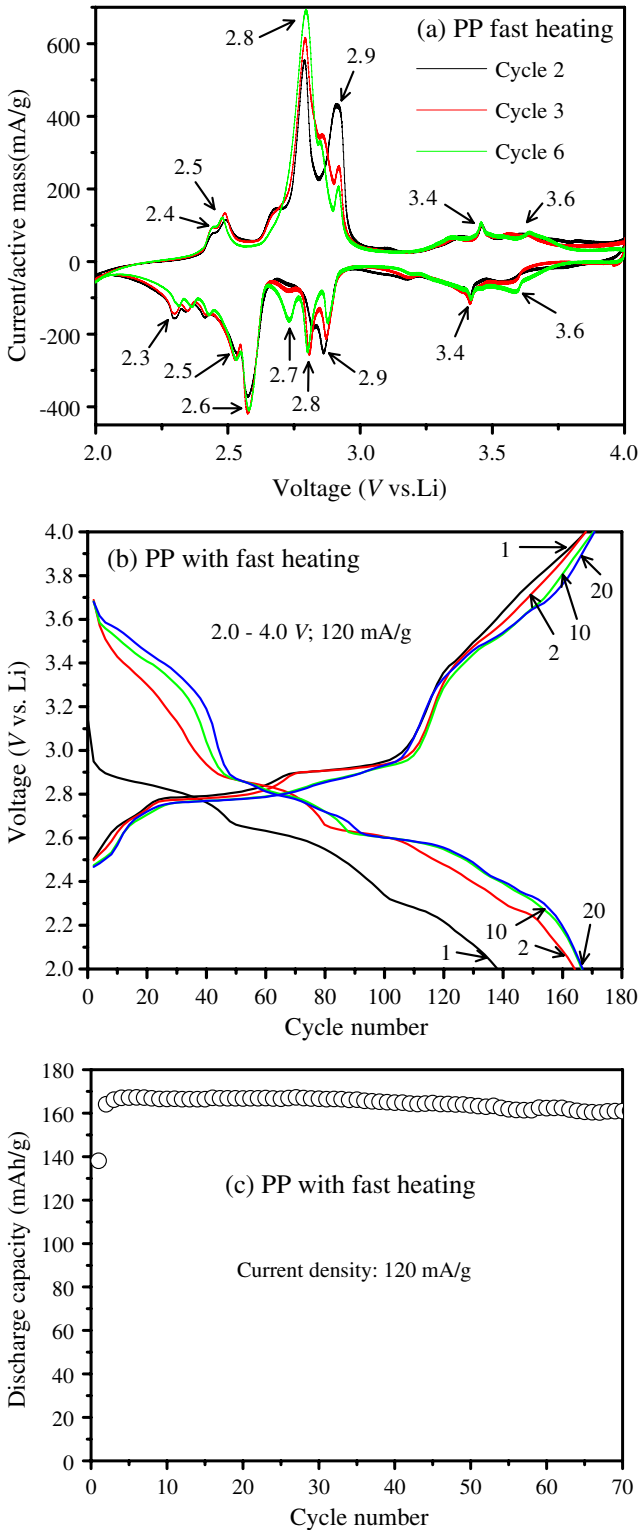

Fig. 6 **a** Cyclic voltammogram at a scan rate of 0.058 mV/s, **b** voltage vs capacity profiles, **c** capacity vs cycle number plot, for the compound prepared by PP method with a faster heating rate. Voltage range, 2.0–4.0 V

corresponds to the 2nd and 70th cycle for the compound prepared by the PP method as shown in Fig. 4c. A notable peak around 2.6 V (encircled) observed in the second cycle was found to be suppressed in the case of the 70th cycle differential plot. This showed that the presence of other active phases had less influence on the electrochemical performance of the LiV_3O_8. It was verified with the results of the compound prepared with more impure phase as discussed in later section. The mechanism of lithium intercalation for the LiV_3O_8 compound during discharge is shown in Eq. 1. The compound in the discharged state is represented by the formula $Li_{1+x}V_3O_8$, with x being the number of intercalated lithium. A reverse reaction takes place during the charging.

$$\text{Discharge}: LiV_3O_8 + xLi^+ + xe^- \rightarrow Li_{1+x}V_3O_8 \qquad (1)$$

The capacity vs cycle number plot is shown in the Fig. 5c. At a current density of 30 mA/g, the compound prepared by the PP method was found to have a second discharge capacity of 208±5 mAh/g (2.23 mol of Li, assuming 93 mAh/g for 1 mol of Li). It shows a capacity retention of 98% at the end of the 70th cycle with a discharge capacity of 203±5 mAh/g (2.18 mol of Li). At a current density of 120 mA/g, the compounds prepared by the SS and PP methods showed a second discharge capacity value of 120±5 mAh/g (1.29 mol of Li) and 140±5 mAh/g (1.50 mol of Li), respectively. The corresponding 70th cycle discharge capacity values were found to be 140±5 mAh/g (1.5 mol of Li) and 170±5 mAh/g (1.83 mol of Li), respectively. This shows that a good cyclic stability has been achieved in both the compounds. The difference between the first charge and discharge capacity or the irreversible capacity loss was found to be 5 and 38 mAh/g for the compounds prepared by the PP and SS methods, respectively. We also noted that the formation cycle continued for more than 45 cycles in case of high-current density. This is due to the micron-sized morphology of the compound leading to diffusion limitations where all the lithium ions might not be able to take part in initial cycling, but with the increase in cycle number, more active material may be participated due to electrochemical grinding, leading to increase in capacity with increase of cycle number. The other reason may be the slight fragmentation of the grains induced by the electrochemical grinding. The smaller grain size reduces the diffusion path for the lithium ions [12]. This could be observed in the galvanostatic cycling studies, where the plateau potentials were shifted to the lower voltages as seen in Fig. 5a, b. It was also clearly reflected in the CV studies at 2nd and 70th cycle (Fig. 4b). Detailed studies on reducing layer thickness by using surfactant-assisted synthesis, rate capability studies, and impedance studies are in progress.

The cyclic voltammograms, galvanostatic charge/discharge cycling curves, and the capacity vs cycle number plot for the compound synthesized by the PP method with a faster heating rate are shown in Fig. 6a, b, and c. The CV at a slow scan rate of 0.058 mV/s was carried up to 6 cycles (Fig. 6a). These results showed that the high intensity peak at 2.6 V during cathodic scan and an anodic/cathodic peak around 3.4 V corresponding to the $Li_{0.3}V_2O_5$ phase was not suppressed at the sixth cycle. In the discharge curve (Fig. 6b), the compound with more impure phases was found to have two well-defined plateau regions, one at around 2.8 V corresponding to the LiV_3O_8 phase and the other at around 2.6 V corresponding to the $Li_{0.3}V_2O_5$ phase, but the compounds by PP and SS methods are found to have only one well-defined plateau region around 2.8 V (Fig. 5a, b). The capacity vs cycle number plot at a current density of 120 mA/g is shown in Fig. 6c. The compound was found to deliver a discharge capacity of 164±5 mAh/g at the end of the second cycle. Capacity retention of 98%

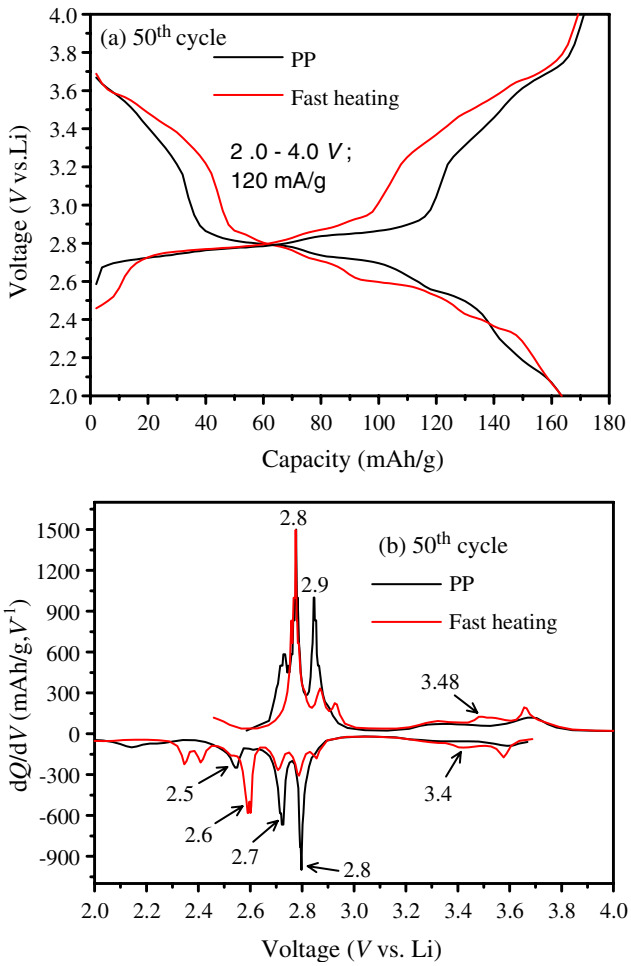

Fig. 7 **a** Voltage vs capacity profiles and **b** differential capacity vs voltage plots corresponding to the 50th discharge/charge cycle for LiV_3O_8 compound prepared by PP method with fast heating rate

was maintained at the end of 70th cycle, with a discharge capacity of 161±5 mAh/g. In comparing the above results with the cycling data of the compound prepared by the PP method at a slow heating rate (Fig. 5c; 120 mA/g), the discharge capacity value was found to coincide at the 50th cycle with a capacity value of 163±5 mAh/g.

The charge/discharge plateaus at the 50th cycle and their corresponding differential plot are shown in Fig. 7a, b. The differential plot of the compound with high percentage of impure phase was found to have a high intensity cathodic peak around 2.6 V and a cathodic/anodic peak around 3.4 V. Both the peaks were fully suppressed for the other compound. As discussed in the CV and differential plot results (Fig. 4) of the compound prepared by the PP method, minor peaks at 2.6 and 3.4 V vs Li appeared initially but then disappeared with the increase in cycle number. This showed that the impure electrochemically active $Li_{0.3}V_2O_5$ or V_2O_5 phases in the present study had no significant influence on the electrochemical performance of the LiV_3O_8 compounds prepared by PP and SS methods.

Figure 8a shows the XRD pattern of the composite electrode made using the LiV_3O_8 compound prepared by the PP method at slow heating rate, before cycling. Figure 8b, c shows the *ex situ* XRD patterns of the composite and cycled electrodes (made using the compounds prepared by the PP method at a slow heating rate) after 70 discharge/charge cycles and the compound prepared at a fast heating rate after six discharge/charge cycles, respectively. The cycled cells were stored for 3 months and subjected to the *ex situ* XRD studies in the charged state (4.0 V). The XRD patterns of the cycled electrodes showed no additional (hkl) lines other than the lines corresponding to the bare compound. The obtained lattice parameter values in the charge state (4.0 V) after 70 cycles were a=6.650 Å, b=3.62 Å, c=12.03 Å, and β=107.55° for the compound prepared by the PP method at a slow heating rate. For the other compound, after 6 cycles, it was found to be a=6.651 Å, b=3.54 Å, c=12.00 Å, and β=107.67°. This showed that no structural modifications took place after cycling. In addition, the XRD pattern of the cycled electrode prepared by the PP method at a fast heating rate showed the appearance of $Li_{0.3}V_2O_5$ phase (Fig. 8c), with a reduced relative intensity when compared to the powder XRD pattern (Fig. 3a). The peak corresponding to the V_2O_5 phase around 2θ=20° was not found clearly, which may be disappeared or overlapped with the broad peak corresponding to the binder and conductive carbon. The $Li_{0.3}V_2O_5$ phase observed in the XRD pattern of the

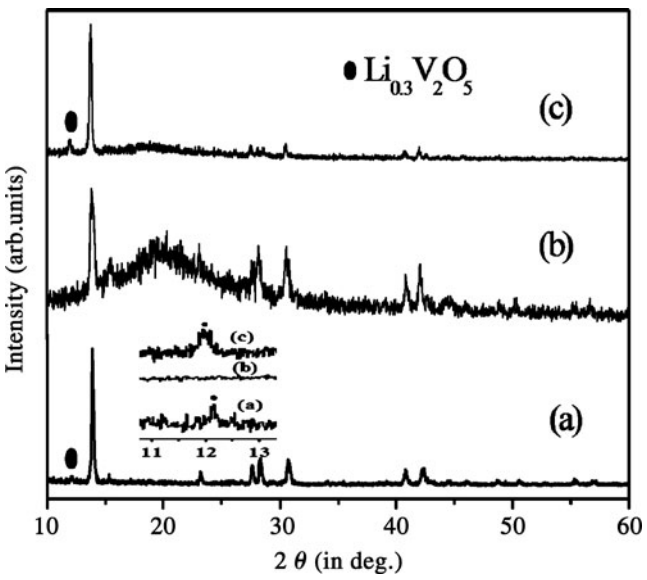

Fig. 8 *Ex situ* XRD pattern of LiV_3O_8 compound prepared by the PP method (slow heating rate), **a** composite electrode before cycling; **b** after 70 galvanostatic cycles in the charged state (4.0 V), and **c** *ex situ* XRD pattern of LiV_3O_8 compound with impure phase of $Li_{0.3}V_2O_5$ and V_2O_5 (fast heating rate) after 6 cycles in the charged state (4.0 V). *Inset* expanded graph between 2θ=11° and 13°

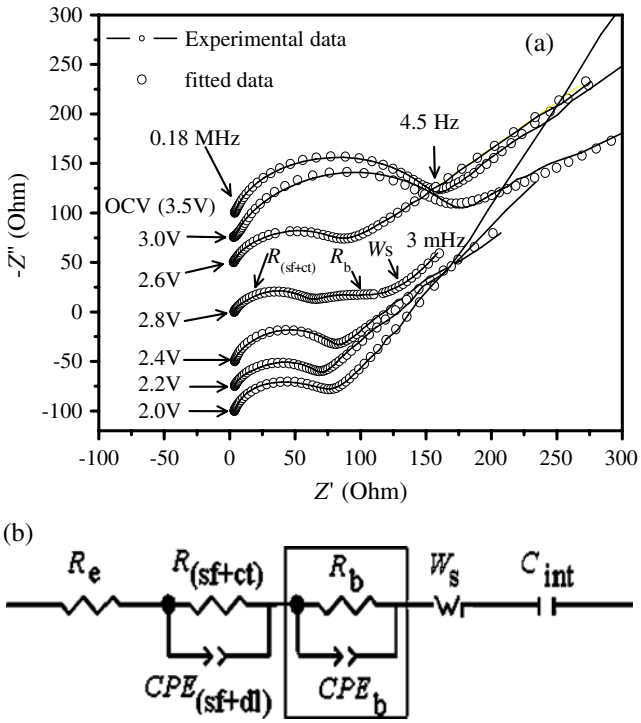

Fig. 9 **a** Nyquist plot (Z' vs.- Z'') of LiV_3O_8 prepared by PP method at different discharge voltages during the first cycle. The semicircles for various discharge voltages are shifted along the y-axis for clarity. And **b** equivalent circuit used to fit impedance spectra. $R_{(sf+ct)}$ is the combined resistance (R) due to the surface film (sf) and charge transfer resistance (ct). $CPE_{(sf+dl)}$ is the corresponding constant phase element due to the surface film and double layer capacitance. R_b is the bulk resistance and CPE_b is the corresponding bulk capacitance. R_e is the electrolyte resistance. W_s is the Warburg resistance, and C_{int} is the intercalation capacitance

composite electrode (Fig. 8a) made from the compound prepared by the PP method at a slow heating rate was found to disappear completely during the electrochemical cycling (Fig. 8b), which is clearly shown in the inset (Fig. 8). The *ex situ* XRD cycling results were found to correlate well with the observed electrochemical studies.

Electrochemical impedance spectroscopy studies

EIS is a well-established technique for the study of electrode kinetics of any electrode materials due to its nondestructive nature and its ability to distinguish various phenomena taking place in an electrode at different time scales [7, 13, 14]. Figure 9a shows the impedance spectra of LiV_3O_8 compound prepared by PP method during selected discharge voltages starting from the open circuit voltage (3.5 V) to 2.0 V. The cells were relaxed at particular voltage for 2 h before each measurement. The impedance spectra showed decrease in impedance with the discharge voltage, and at 2.8 V, a small semicircle in the low frequency region corresponding to the bulk resistance was observed. The impedance spectrum for the 2.8 V was fitted using the equivalent circuit represented in the Fig. 9b. The proposed circuit and the assignment of R_i/CPE_i are in conformity with the recent trends in the interpretation of impedance spectra of electrode materials [7, 12, 13, 15, 16]. R_i and CPE_i (i = sf, ct, b, or dl) denote the resistance and the corresponding constant phase element due to different parameters like surface film resistance and capacitance (R_{sf}, CPE_{sf}), charge transfer resistance and double layer capacitance (R_{ct}, CPE_{dl}), and bulk resistance and capacitance (R_b, CPE_b) phenomena taking place in the cell. For all the other discharge voltages, the spectra were fitted using the one equivalent circuit model without including the bulk resistance. At OCV, the R_{sf} and CPE_{sf} values were 138±3 Ω and 24±3 μF, respectively. The resistance value was found to be less than 100 Ω for voltages below 3.0 V, and the capacitance value was in the range of microfarad. For the discharge voltages of 3.0, 2.8, 2.6, 2.4, 2.2, and 2.0 V, the resistance ($R_{(sf+ct)}$) and the capacitance ($CPE_{(sf+dl)}$) values were 127, 55, 76, 68, 65, 73 (±3) Ω and 30, 122, 74, 39, 108, and 134 (±3) μF, respectively. The bulk resistance (R_b) at the 2.8 V was found to be 60 Ω with corresponding bulk capacitance (CPE_b) value of 10 mF. The decrease in impedance with the discharge voltage indicates the smooth intercalation of lithium ions in the compound. The straight line that is inclined at an angle of 45° at the end of the semicircle corresponds to the finite length Warburg resistance (W_s), which is related to the solid state diffusion. The low-frequency region after Warburg resistance corresponds to the intercalation capacitance (C_{int}). The resistance due to electrolyte and the cell components are 3 to 5 Ω, and the C_{int} is ~0.1–0.5 F.

Conclusions

LiV_3O_8 have been prepared by a simple polymer precursor method and characterized by various techniques. LiV_3O_8 showed a good reversible capacity of 203±5 mAh/g (2.2 mol of Li) at the end of the 70th cycle at a current density of 30 mA/g. Minor electrochemically active impure phases of $Li_{0.3}V_2O_5$ and V_2O_5 in LiV_3O_8 compound did not have much influence on the discharge capacity values. The good electrochemical stability achieved shows that LiV_3O_8 could be used as a 2.8 V cathode material for lithium batteries.

Acknowledgment Authors thank Prof. G.V. SubbaRao for his helpful discussions. One of the authors, A. Sakunthala, thanks the Defence Research and Development Organization (DRDO), India, for providing the Senior Research Fellowship. Dr. M.V. Reddy, Prof. B.V.R. Chowdari thank the Ministry of Education (MOE), Singapore.

References

1. Chew SY, Sun JZ, Wang JZ, Liu HK, Forsyth M, MacFarlane DR (2008) Electrochim Acta 53:6460
2. West K, Zachau Christiansen B, Skaarup S, Saidi Y, Barker J, Olsen II, Pynenburg R, Koksbang R (1996) J Electrochem Soc 143:820
3. Kannan AM, Manthiram A (2006) J Power Sources 159:1405
4. Patey TJ, Ng SH, Buchel R, Tran N, Krumeich F, Wang J, Liu HK, Novak P (2008) Electrochem & Solid-state Lett 11:A46
5. Gao J, Jiang CY, Wan CR (2004) J Power Sources 125:90
6. Liu HM, Wang YG, Wang KX, Wang YR, Zhou HS (2009) J Power Sources 192:668
7. Reddy MV, Subba Rao GV, Chowdari BVR (2007) J Phys Chem C 111:11712
8. Wang GJ, Zhao NH, Yang LC, Wu YP, Wu HQ, Holze R (2007) Electrochim Acta 52:4911
9. Jouanneau S, La Salle AL, Verbaere A, Deschamps M, Lascaud S, Guyomard D (2003) J Mater Chem 13:921
10. Bonino F, Panero S, Pasquali M, Pistoia G (1995) J Power Sources 56:193
11. Deptula A, Dubarry M, Noret A, Gaubicher J, Olczak T, Lada W, Guyomard D (2006) Electrochem & Solid-state Lett 9:A16
12. Liu YM, Zhou XC, Guo YL (2009) Electrochim Acta 54:3184
13. Aurbach D, Markovsky B, Weissman I, Levi E, Ein-Eli Y (1999) Electrochim Acta 45:67
14. Nobili F, Croce F, Scrosati B, Marassi R (2001) Chem Mater 13:1642
15. Das B, Reddy MV, Krishnamoorthi C, Tripathy S, Mahendiran R, Subba Rao GV, Chowdari BVR (2009) Electrochim Acta 54:3360
16. Reddy MV, Yu T, Sow CH, Shen ZX, Lim CT, Subba Rao GV, Chowdari BVR (2007) Adv Func Mater 17:2792